Journal of Orthopaedic Translation (2018) 12, 6—15

Available online at www.sciencedirect.com

ScienceDirect

journal homepage: http://ees.elsevier.com/jot

ORIGINAL ARTICLE

A novel gait-based synthesis procedure for the design of 4-bar exoskeleton with natural trajectories

Ramanpreet Singh*, **Himanshu Chaudhary**, **Amit K. Singh**

Department of Mechanical Engineering, Malaviya National Institute of Technology, Jaipur, 302017, India

Received 27 June 2017; received in revised form 20 September 2017; accepted 21 September 2017
Available online 20 November 2017

KEYWORDS
Exoskeleton;
Four-bar;
Gait-based synthesis;
Lower limb

Abstract *Background/Objective:* Human walking involves the coordination of brain, nerves, and muscles. A disturbance in their coordination may result in gait disorder. The gait disorder may be treated through manually assisted gait training or with the aid of assistive devices/robotic devices. These robotic devices involve mechanisms which are synthesized using complex conventional procedures. Therefore, in this study, a new gait-based synthesis procedure is proposed, which simplifies the mechanism synthesis and helps to develop a mechanism which can be used in rehabilitation devices, bipeds, etc.
Methods: This article presents a novel procedure for the synthesis of 4-bar linkage using the natural gait trajectories. As opposed to the conventional synthesis procedures, in this procedure, a global reference frame is considered, which allows the use of hip trajectory while moving. Moreover, this method is divided into two stages, and five precision points are considered on the hip trajectory in each stage. In the first stage, the 4-bar linkage is designed, thereafter, the configurations of the linkage for the remaining precision points are determined in the second stage. The proposed synthesis procedure reduces the complexity involved in the synthesis and helps in the simplification of the problem formulation. A two-stage optimization problem is formulated for minimizing the error between the generated and desired hip trajectories. Two nature-inspired algorithms are used for solving the optimization problem. The obtained best results are presented, and the designed linkage is simulated in MATLAB.
Results: The best design of the linkage is obtained using particle swarm optimization. The trajectories generated by the designed linkage using the proposed methodology can accurately track the desired path, which indicates that designed linkage can achieve all the orientations required during walking. The positions of a whole lower limb at all the desired precision points are demonstrated by stick diagram for one gait.
Conclusion: The proposed methodology has reduced the complexity of synthesis procedures and used optimization techniques to obtain a feasible design of the mechanism. The stick

* Corresponding author. Department of Mechanical Engineering, Malaviya National Institute of Technology, JLN Marg, Jaipur, India.
E-mail address: ramanpreet.gurdutta@hotmail.com (R. Singh).

https://doi.org/10.1016/j.jot.2017.09.001
2214-031X/© 2017 The Authors. Published by Elsevier (Singapore) Pte Ltd on behalf of Chinese Speaking Orthopaedic Society. This is an open access article under the CC BY-NC-ND license (http://creativecommons.org/licenses/by-nc-nd/4.0/).

diagram of the designed mechanism obtained using the proposed method indicates that the designed mechanism can walk smoothly. Hence, the designed mechanism can be used in the rehabilitation devices. Furthermore, a conceptual design of an exoskeleton knee is also presented.

The Translational Potential of this Article: Many hospitals and individuals have used the immobile and portable rehabilitation devices. These devices involve mechanisms, and the design of mechanism plays a vital role in the functioning of these devices; therefore, we have developed a new synthesis procedure for the design of the mechanism. Besides synthesis procedure, a mechanism is developed that can be used in the rehabilitation devices, bipeds, exoskeletons, etc., to benefit the society.

© 2017 The Authors. Published by Elsevier (Singapore) Pte Ltd on behalf of Chinese Speaking Orthopaedic Society. This is an open access article under the CC BY-NC-ND license (http://creativecommons.org/licenses/by-nc-nd/4.0/).

Introduction

Human walking is a complicated and rhythmic kinematic movement which involves the coordination of brain, nerves, and muscles. A disturbance in their coordination may result in gait disorder [1]. Typically, it is found among elderly patients who have amputated limbs, musculoskeletal disorders, spinal cord injury, etc. These patients may be treated by manually assisted gait training or with the aid of assistive devices. The manually assisted gait training has various drawbacks such as the long training duration and its frequency of the training. It is also dependent on the availability of the therapist. Moreover, it is backbreaking and physically demanding for the therapists, and lacks repeatability [2,3].

In contrast, robot-assisted gait training (i.e. assistive device) can be used to increase the duration and number of sessions for training. In addition, it limits the requirement of the number of therapists per patient [4]. These assistive devices may be used to overcome the limitations of manually assisted gait training [5]. Various gait rehabilitation devices have been developed over the years such as Lokomat [3], ReoAmbulator [6], LOPES [7], ALEX [8], linkage mechanism for gait rehabilitation [2], and UCI gait mechanism [9]. However, these devices are meant for patients at hospitals and rehabilitation centres as they provide training in the confined areas, and patients do not feel the realistic experience of walking. Alternatively, portable wearable robots are required, which can be used at home. Various portable rehabilitation devices have been developed, for example, eLEGS [10], compact portable Knee—Ankle—Foot robot [4], and ReWalk [11]. These devices may be used to assist patients in standing and walking. However, these exoskeletons are battery operated, and some of them require crutches for balance [12,13]. In addition, they use a single-axis, revolute joint at the knee, which allows only rotational motion. Therefore, to select the best mechanism, it is vital to comprehend the biomechanics of the knee joint and its coordination with the hip and ankle joints.

The anatomy of knee joint varies with age, whereas its complex function remains constant. The knee joint is also referred as a gliding hinge joint. It offers six-degree of freedom range of motion, which involves three rotational and three translational movements. Flexion—extension, internal—external, and varus-valgus movements come under rotation, whereas anterior-posterior, medial-lateral, and compression—distraction movements come under translation [14]. The experimental trials of the rehabilitation devices such as Lokomat clarify the fact that ankle trajectory can be considered as planar in sagittal plane [2,3]. Rolling and gliding are the key motions of the knee joint in the sagittal plane. Also, they are considered as the basic mechanism of movement between femur and tibia as shown in Figure 1. This kinematic motion of the knee joint can be achieved through cross 4-bar linkage where anterior cruciate and posterior cruciate ligaments can be considered as rigid links [15,16]. The 4-bar linkage allows the combination of rotation and translation motion of the knee joint in sagittal plane [17]. Also, it has been used for the knee joint of bipedal robots [17—20] and prosthetic knee joints [21]; therefore, to imitate the complex function of the knee joint for creating orthotic and rehabilitation devices, a 4-bar mechanism can be used.

Various gait rehabilitation devices and exoskeletons are available, in which different mechanisms have been used for the knee, ankle, and hip joints. Recently, a linkage design gait trainer (LGT) has been developed which used a 4-bar linkage mechanism to generate normal gait trajectories. It combines a commercially available walker with linkage system which makes the LGT device complex [22]. A revolute joint is typically used at the knee in the portable active orthotic device [23]. However, it does not imitate the complex

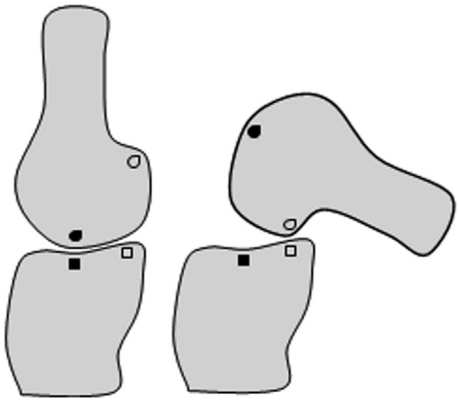

Figure 1 Contact points generated while rolling and gliding motion, when femur moves relative to tibia.

function of the knee joint. In contrast, the 4-bar linkage is found suitable for the portable gait exoskeleton [24], and it can be used for the exoskeleton knee to augment the load-carrying capacity [25]. The design can be improved by adding an elastic element to the 4-bar linkage [26]. The slider-crank mechanism can also be used at the knee and ankle joints [4,27]. In addition to the 4-bar mechanism, 6-bar [21] and the 8-bar leg mechanisms [28] can also be used for the gait rehabilitation. Apart from the kinematic aspects of synthesis, static and kinematic synthesis can be combined to get a realistic mechanism [29]. It has been found that procedures of mechanism synthesis for the knee joint of the portable gait rehabilitation robots and orthotic devices have been relatively less explored.

Typically, mechanisms for gait rehabilitation or assistive devices are synthesized by taking an ankle trajectory in shape of a "tear drop." This happens by transforming the coordinates of ankle joint relative to the hip joint because it is believed that the synthesis procedure requires the hip joint to be stationary [30]. Various gait rehabilitation and assistive devices have been developed using this theory, for example, UCI gait mechanism [9], linkage gait rehabilitation system [2], LGT device [22], 10-bar linkage to guide gait [31], and lower extremity wearable device [32]. In contrast, mechanisms are also synthesized using the flexion/extension trajectory of the human knee [24]. This concept has been used extensively in the design of prosthetic knee joints and bipeds. However, these conventional synthesis procedures require the solution of complex equations and use less number of precision points. Therefore, the generated trajectory is not accurate. There is a need to simplify the synthesis procedure for the design of gait rehabilitation/exoskeleton devices by considering *N*-precision points, which can improve the path-tracing ability of mechanism. It is observed that some mechanisms have used revolute joints for the knee of exoskeleton lower limb, whereas others have used 4-bar and 6-bar mechanisms. The synthesis procedure of those mechanisms requires the hip joint to be stationary and involves the solution of complex equations.

Therefore, a 4-bar mechanism is proposed in this article to replace the single-axis revolute joint in the knee—ankle—foot, hip—knee—ankle-foot, and knee orthoses. Since the conventional synthesis procedures, require the solution of complex equations and use less number of precision points, which results in inaccurate trajectory tracking. Thus, a novel gait-based mechanism synthesis procedure for *N*-precision points has been proposed to design a mechanism, which can be embedded in the orthotic and portable gait rehabilitation devices. In this study, rather than considering the conventional procedure (stationary hip joint) for the mechanism synthesis, a global reference frame has been taken to synthesize the 4-bar mechanism for the *N*-precision points. The expressions of trajectories are derived, and a two-stage optimization method is proposed to synthesize the linkage in the first stage followed by position synthesis by controlling angles in the second stage. The two-stage optimization method minimizes the error between generated and desired hip trajectories. The generated hip trajectories can accurately track the path, and the synthesis equations are simplified. The simulation is performed in MATLAB and is demonstrated as stick diagram.

The remainder of the article is structured as follows: Methods section describes the process of selection of precision points, kinematic modeling of the 4-bar exoskeleton lower limb, and optimization problem formulation. Results section describes a numerical example, results, and their validation. Finally, Discussions are outlined in the last section.

Methods

Selection of precision points

A set of data points of the hip and ankle joints of a healthy participant walking on a leveled surface is taken from the *MNIT gait database* [33]. The data set marks the hip and ankle joints' positions for two gait cycles of the same lower limb as shown in Figure 2A. The position coordinates are collected in the global reference frame where hip joint is moving. In the conventional synthesis procedures, the hip joint requires to be stationary, and the data are transformed relative to the hip joint. In contrast, here the trajectories are taken with respect to the global reference frame. The x-direction is taken as positive toward the right of the origin, and the y-direction, that is, from shoulder to ankle is taken as negative. The original data are taken in pixel and are calibrated to millimeters (mm). The red (in the web version) markers in Figure 2B indicate the positions of ankle and hip joints. The hip positions (x-coordinate) indicate that participant moves from 3685.9 mm toward 525.4545 mm, that is, from the positive right toward origin as shown in Figure 2. However, in this study, to comprehend the mathematical model with ease, the linkage is moved from the negative left toward origin as shown in Figure 4B. Therefore, x-coordinates are transformed accordingly and are presented in Table 1. "Best-fit" curves which fit 68 data points for desired and input trajectories of hip and ankle joints, respectively, are identified using MATLAB (MathWorks, United States).

It is difficult to use all the 68 data points as precision positions to synthesize the linkage. Therefore, 10 precision points are selected (Table 1) of 68 data points, using scheme presented in Figure 3, for one gait cycle to synthesize a mechanism. To select the precision points, parametric equations of best-fit curves for the ankle (A_{xd}, A_{yd}) and the hip joints (P_{xd}, P_{yd}) are formed using MATLAB. The equations are evaluated at an equal interval of 166.3397 and 165.933 mm for hip and ankle joints, respectively, for 20 precision points of two gait cycles. These intervals are selected based on the start and end points of the X-coordinate, which are 3685.9 and 525.4545 mm for the hip joint, and 3685.9 and 533.1818 mm for ankle joint, respectively. The scheme for selection of the precision points is shown in Figure 3.

Kinematic modeling of four-link exoskeleton

In this section, lower limb exoskeleton is modeled as a 4-bar linkage, shown in Figure 4A, in which, links #1 and #3 are fixed to the shank and the thigh, respectively. Other links #2 and #4 connect links #1 and #3 to form the closed loop *CDFE* of the linkage. This exoskeleton 4-bar linkage defined by four links #1, #2, #3, and #4 are denoted by CD, CE, EF, and DF, respectively. Note that *GP* and *BA* are

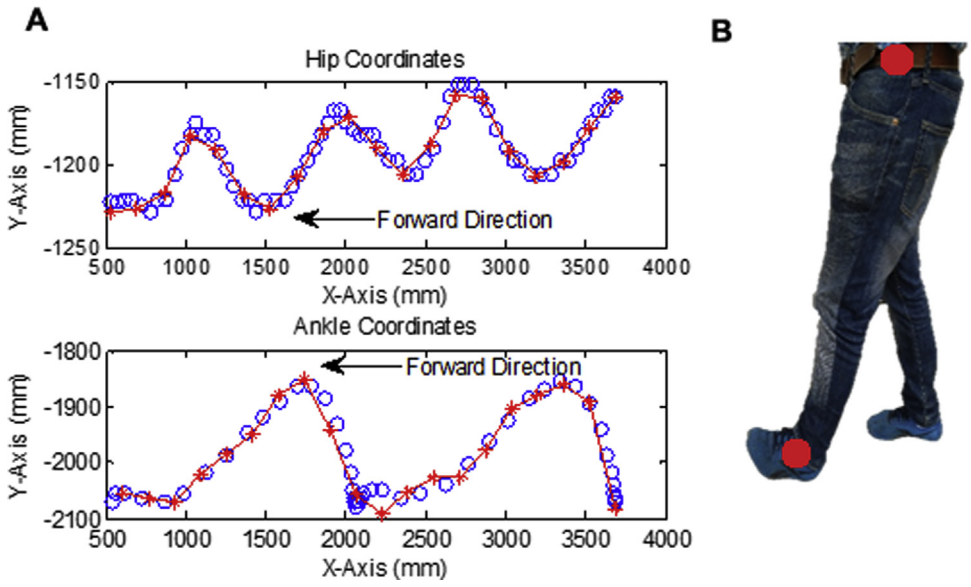

Figure 2 (A) Curve fitting of the trajectory data and (B) marker indicating hip and ankle positions.

extensions of links *EF* and *CD* along thigh and shank, respectively. Also, note that points *P* and *A* represent hip and ankle joints, respectively. The links' lengths and their orientation with respect to the *X*-axis are denoted by r_1, r_2, r_3, and r_4, and $(270^o + \theta_1), \theta_2, \theta_3$, and θ_4, respectively, as shown in Figure 4B. Lengths of the extended links *AB* and *GP* are taken as l_1 and l_2, respectively, which are oriented 90° to *CD* and *EF*, respectively, at the center of their links. The ankle and hip trajectories are taken from real *Gait database* [33]. The ankle trajectory is used as input to synthesize the linkage which tracks the given hip trajectory. Here, the linkage is assumed to move in the sagittal plane, as shown in Figure 4.

The linkage *CDFE* forms a closed loop, where θ_1 and θ_2 are the unknown angles for one gait cycle. Whereas, the orientations θ_3 and θ_4 of links *EF* and *FD*, respectively, can be determined by loop-closure equation of linkage.

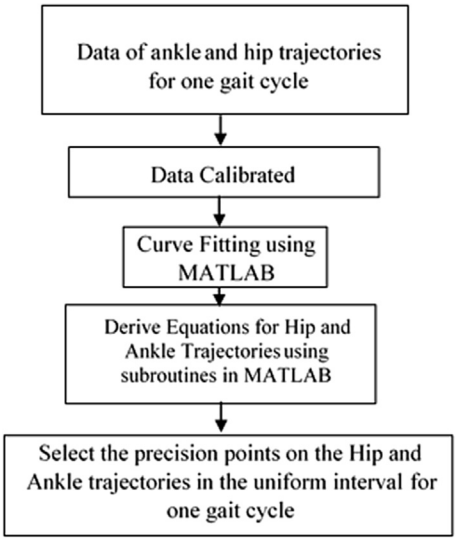

Figure 3 Scheme for selection of precision points.

Therefore, to obtain the configuration of 4-bar linkage, the loop-closure equation is required to be solved [34]. The details for solving the loop-closure equation are provided in Appendix 1. Here, the coordinates of ankle $A(A_{xd}, A_{yd})$ are taken as input and the coordinates C, E, G, and P are derived in global frame *XOY*, which can be expressed as:

$$B_x = A_{xd} + l_1 \cos(\theta_1) \tag{1}$$

$$B_y = A_{yd} + l_1 \sin(\theta_1) \tag{2}$$

$$C_x = B_x + \frac{r_1}{2}\cos\left(\frac{\pi}{2} + \theta_1\right) \tag{3}$$

$$C_y = B_y + \frac{r_1}{2}\sin\left(\frac{\pi}{2} + \theta_1\right) \tag{4}$$

$$E_x = C_x + r_2 \cos(\theta_2) \tag{5}$$

$$E_y = C_y + r_2 \sin(\theta_2) \tag{6}$$

$$G_x = E_x + \frac{r_3}{2}\cos(\theta_3) \tag{7}$$

$$G_y = E_y + \frac{r_3}{2}\sin(\theta_3) \tag{8}$$

The trajectory of the point *P* is obtained using Eqs. (1)–(8), which is expressed as follows:

$$P_x = G_x + l_2 \cos\left(\frac{\pi}{2} + \theta_3\right) \tag{9}$$

$$P_y = G_y + l_2 \sin\left(\frac{\pi}{2} + \theta_3\right) \tag{10}$$

These trajectories can be used for the dimensional synthesis of the 4-bar linkage for the lower limb exoskeleton. The design parameters r_1, r_2, r_3, r_4, l_1, and l_2 and the orientation of the extended link *AB and* the link *CE* with

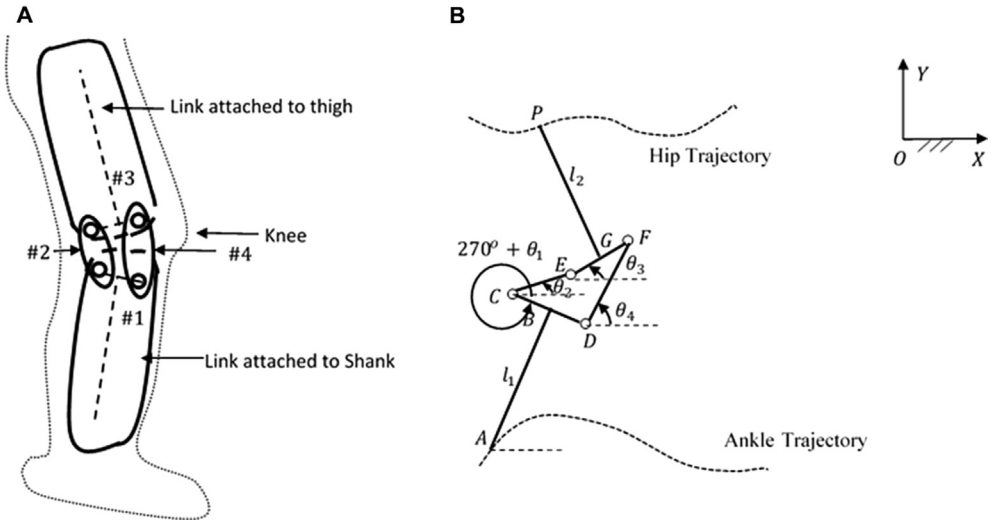

Figure 4 (A) Four-link exoskeleton for lower limb and (B) various definitions for four-link exoskeleton.

respect to X-axis are unknowns. These parameters can be determined using a two-stage optimization formulation proposed in the next section.

Two-stage optimization problem formulation

This section proposes a novel two-stage optimization problem formulation to find the optimal value of design parameters of 4-bar linkage as discussed in Kinematic modeling section. Here, 4-bar linkage synthesis is formulated as an optimization problem. The 4-bar linkage synthesis can be performed by considering a single stage of optimization procedure for $2N$ precision points with $4N+6$ design variables, r_1, r_2, r_3, r_4, l_1, l_2, θ_1^k, and θ_2^k, where $k=1,\ldots,N$ positions. A large number of design variables increase complexity of the optimization problem to get satisfactory results. Therefore, to reduce the complexity of the optimization and to simplify the linkage synthesis procedure, the linkage synthesis problem is divided into two stages. For $2N$-precision points synthesis, in the first stage, linkage synthesis is performed by considering $N-$ precision points with $2N+6$ design variables, r_1, r_2, r_3, r_4, l_1, l_2, θ_1^k, and θ_2^k, where $k=1,\ldots,N$ positions. In this stage, link's lengths, r_1, r_2, r_3, r_4, l_1, l_2, and input angles θ_1^k and θ_2^k, where $k=1,\ldots,N$ precision points are determined. The next $N-$ precision points will be obtained by controlling only θ_1^k and θ_2^k, where $k=N+1,\ldots,2N$. These controlling angles are determined in the second stage of optimization. Hence, these two stages reduce the complexity of the linkage synthesis procedure and provide satisfactory results. A complete scheme of the two-stage optimization algorithm

Table 1 Selected precision points on the fitting curve.

Positions	$P_{xd} * 1000$	$P_{yd} * 1000$	$A_{xd} * 1000$	$A_{yd} * 1000$
1	−3.6859	−1.1590	−3.6859	−2.0826
2	−3.5196	−1.1775	−3.5236	−1.8906
3	−3.3532	−1.1981	−3.3614	−1.8590
4	−3.1869	−1.2071	−3.1991	−1.8783
5	−3.0206	−1.1919	−3.0368	−1.9024
6	−2.8542	−1.1600	−2.8745	−1.9767
7	−2.6879	−1.1577	−2.7123	−2.0273
8	−2.5215	−1.1878	−2.5500	−2.0288
9	−2.3552	−1.2052	−2.3877	−2.0509
10	−2.1889	−1.1900	−2.2255	−2.0918

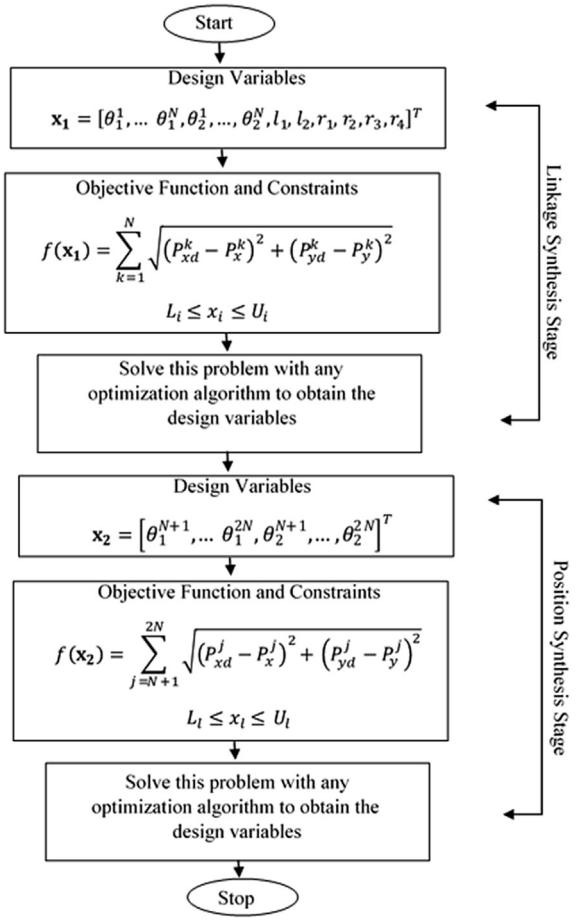

Figure 5 Scheme of two-stage optimization problem.

is shown in Figure 5. The objective functions and design variables involved in both the stages are as follows:

First stage (linkage synthesis)
The first stage is the linkage synthesis stage, where the first N precision points are considered. The goal of the first objective function is to track these N precision points where each point involves a set of unknown parameters $\theta_1^k, \theta_2^k, l_1, l_2, r_1, r_2, r_3$, and r_4. These independent parameters are considered as design variables, in which $k=1,\ldots,N$. Note that the angles θ_3^k and θ_4^k corresponding to each position of θ_1^k and θ_2^k are determined through loop-closure equation of the 4-bar linkage (Appendix 1). For $N-$ precision points' synthesis, a total of $2N+6$ variables is required, where θ_1^k and θ_2^k constitute $2N$ variables and links' dimensions constitute six variables.

Design variables (first stage)
The design vector in the first stage of the optimization problem can be expressed as:

$$\mathbf{x}_1 = \left[\theta_1^1,\ldots\theta_1^N, \theta_2^1,\ldots,\theta_2^N, l_1, l_2, r_1, r_2, r_3, r_4\right]^T \tag{11}$$

Objective function (first stage) and constraint
In this stage, the error between generated and desired hip trajectories (point P) is considered as the objective function for the input foot trajectory (point A). The desired hip and input foot trajectories are shown in Table 1, and the hip trajectory (generalized) traced by the point P is shown in Figure 4. The error minimization objective between the desired and generated trajectories can be expressed as:

$$f(\mathbf{x}_1) = \sum_{k=1}^{N} \sqrt{\left(P_{xd}^k - P_x^k\right)^2 + \left(P_{yd}^k - P_y^k\right)^2} \tag{12}$$

The bound constraints are applied to the design variables to get a feasible solution

$$L_i \le x_i \le U_i$$

Finally, the optimization problem can be stated as:

$$\text{Minimize}: f(\mathbf{x}_1) = \sum_{k=1}^{N} \sqrt{\left(P_{xd}^k - P_x^k\right)^2 + \left(P_{yd}^k - P_y^k\right)^2} \tag{13}$$

Subject to $L_i \le x_i \le U_i$; $i=1,\ldots,n_1$.

Where, L_i and U_i are the lower and the upper bounds on the i^{th} design variable, n_1 is the total number of design variables in the first stage, k is the k^{th} position achieved by link #3 in the first stage.

The first stage is completed after the determination of the linkage design, which can track the hip trajectory with minimum error. Then, the position synthesis for the remaining cycle is performed in the second stage.

Second stage (position synthesis)
Linkage dimensions are not considered as design variables in the second stage as these are determined in the first stage. If the linkage dimensions are kept as design variables for the second stage, then optimization would result in a new linkage design. Therefore, in this stage, only positions are synthesized by controlling angles θ_1^k and θ_2^k.

Design variables (second stage)
The $2N$ variables $\theta_1^1,\ldots\theta_1^k, \theta_2^1,\ldots,\theta_2^k$, where $k=N+1,\ldots,2N$ are considered as design variables and can be expressed as:

$$\mathbf{x}_2 = \left[\theta_1^{N+1},\ldots\theta_1^{2N}, \theta_2^{N+1},\ldots,\theta_2^{2N}\right]^T \tag{14}$$

Objective function (second stage) and constraints
The objective is to synthesize the linkage positions that can track all the precision points with minimum error. Therefore, an error minimization problem is formulated to tracking the desired hip trajectory while using the linkage design obtained in the first stage. Thus, the minimization error function can be expressed as:

$$f(\mathbf{x}_2) = \sum_{j=N+1}^{2N} \sqrt{\left(P_{xd}^j - P_x^j\right)^2 + \left(P_{yd}^j - P_y^j\right)^2} \tag{15}$$

The bound constraints are applied to the design variables to generate the desired hip trajectory with least error.

$$L_l \le x_l \le U_l$$

Finally, the optimization problem can be posed as:

$$\text{Minimize}: f(\mathbf{x}_2) = \sum_{j=N+1}^{2N} \sqrt{\left(P_{xd}^j - P_x^j\right)^2 + \left(P_{yd}^j - P_y^j\right)^2} \tag{16}$$

Subject to $L_l \le x_l \le U_l$, $l=1,\ldots,n_2$

Where L_l and U_l are the lower and the upper bounds on the l^{th} design variable, n_2 is the total number of design variables in the second stage, j is the j^{th} position achieved by link #3 in the second stage.

Results

Numerical example

In this section, a realistic numerical example is included to demonstrate the effectiveness of the two-stage algorithm as defined in the preceding section. A 4-bar linkage exoskeleton is synthesized using the proposed design procedure for lower limb of the participant of age 20 years, height 1.70 m, weight 54 kg, and leg length of 0.92 m. The foot and hip trajectories of the healthy participant are taken from gait database [33], and 10 precision points are selected on one gait cycle. The detailed procedure for selection of the precision points on the desired and input trajectories is illustrated in the Methods section.

The first five precision points are taken in the first stage synthesis, in which θ_1^k and θ_2^k, where $k=1,\ldots,5$, and r_1, r_2, r_3, r_4, l_1, and l_2 are design variables. The bounds on the design variables which are taken as follows:

First stage:

$$\theta_1^k \in \left[0, \frac{\pi}{2}\right], \theta_2^k \in [0, 2\pi], r_1, r_2, r_3, r_4 \in [40, 170], l_1 \in [280, 500],$$
$$l_2 \in [280, 400]$$

Second stage:

$$\theta_1^k \in \left[0, \frac{\pi}{2}\right], \theta_2^k \in [0, 2\pi]$$

Note that the angle is in radian and length is in mm.

To obtain a feasible solution, the two well-established algorithms, namely, teaching-learning-based optimization (TLBO) and particle swarm optimization (PSO) are used. The purpose of using two-nature inspired algorithms is not to compare their performance, but to validate their results, which should be near approximate of the global minimum. Because both these nature-inspired algorithms are stochastic in nature, therefore, each algorithm is run 25 times, and the best solution with minimum error is selected which is as follows:

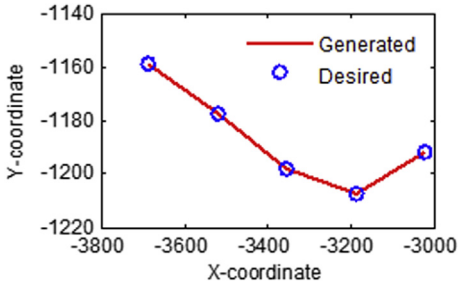

Figure 7 Generated trajectory and desired points of hip joint *P* during the first stage using PSO.

$$\mathbf{x}_1 = \begin{bmatrix} 1.2374, 0.7530, 0.6750, 0.6825, 0.7323, 1.6622, 2.4527, 2.6601, \\ 2.6131, 2.4457, 471.0019, 374.0438, 72.4620, 104.4731, 123.6035, 119.0642 \end{bmatrix}^T$$

Figure 6 shows that PSO converges faster and gives less error in comparison with TLBO in the first stage of the algorithm. The best linkage obtained by PSO tracks all five precision points accurately as shown through Figures 6–8.

Thereafter, the designed linkage is used further for tracking remaining five precision points on the hip trajectory. The position (configuration) synthesis is performed during the second stage of the algorithm. The same procedure is used for solving the optimization algorithm as used in the first stage. Figure 9 shows that PSO converges faster than TLBO in the second stage. The design vector of the synthesized positions for the linkage is obtained using PSO in the second stage. The resulted design vector is as follows:

Figure 10 shows the trajectory generated by designed linkage tracks the remaining five precision points accurately. Also, the configuration of the designed linkage while moving is shown in Figure 11. Lastly, the stick diagram in Figure 12 shows that the 4-bar linkage designed using the proposed synthesis procedure can track all the precision points for one gait cycle. Moreover, it also demonstrates the configurations of the lower limb (4-bar linkage) at each desired precision point. If this linkage is fixed to a user, their lower limb can generate the appropriate trajectories required for one gait cycle. Therefore, the designed linkage can be used for any application which requires walking.

$$\mathbf{x}_2 = [0.9179, 1.0401, 0.9637, 0.9705, 1.1220, 1.9755, 1.7669, 1.8648, 1.8414, 1.6623]^T$$

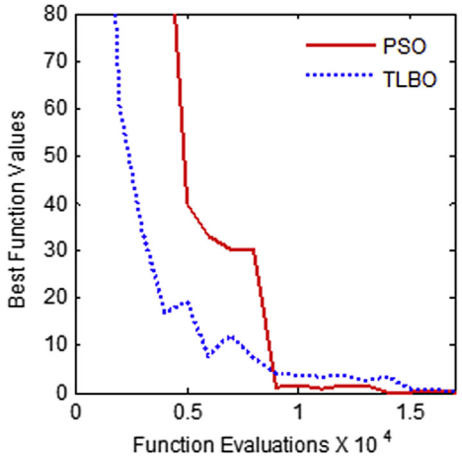

Figure 6 Convergence of best objective function versus number of function evaluations.

Discussions

In the conventional mechanism synthesis procedure, the experimental data are required to transform relative to hip which appears as a "tear-drop" trajectory. Moreover, they involve the solution of complex equations while synthesizing a mechanism. These procedures are less accurate because they use less number of precision points for synthesis. Hence, there is a need to simplify the synthesis procedure for the design of gait rehabilitation and orthotic devices to improve the path tracing ability of mechanisms. Therefore, to resolve these issues, a gait-based synthesis procedure is proposed in this article.

A 4-bar mechanism is also proposed in this article, which can be used to replace the single-axis revolute joint in the knee–ankle–foot, hip–knee–ankle-foot, and knee orthoses. Thus, the design obtained using the simplified gait-based mechanism synthesis procedure can be embedded in

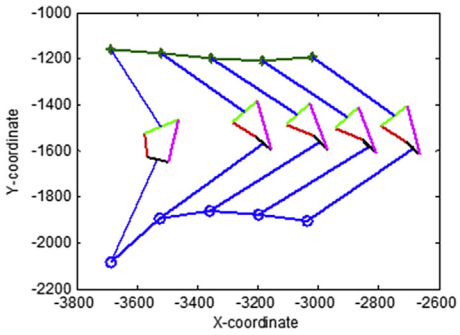

Figure 8 Tracking of precision points on the hip trajectory.

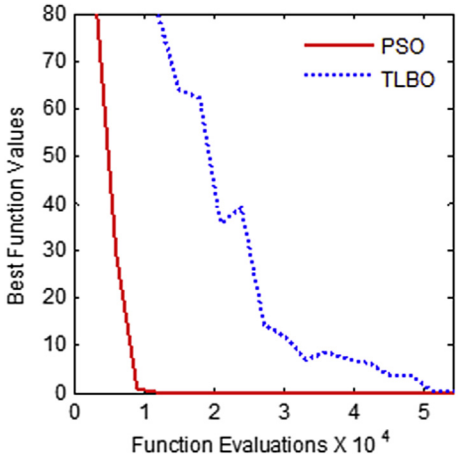

Figure 9 Convergence of best objective function versus number of function evaluations.

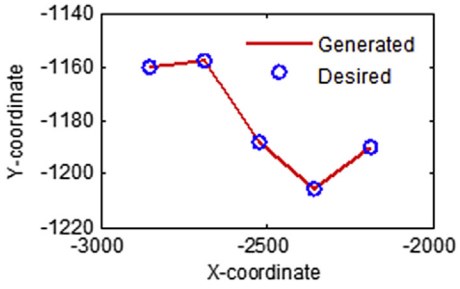

Figure 10 Generated trajectory and desired points of hip point *P* during the second stage using PSO. PSO, particle swarm optimization.

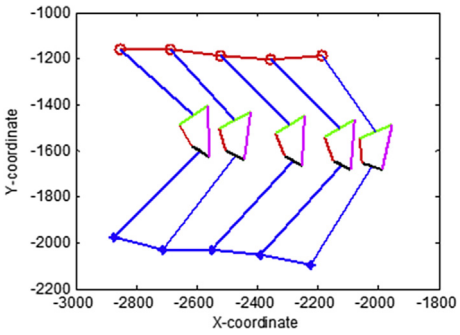

Figure 11 Four-bar linkage lower limb tracking five precision points on the hip trajectory.

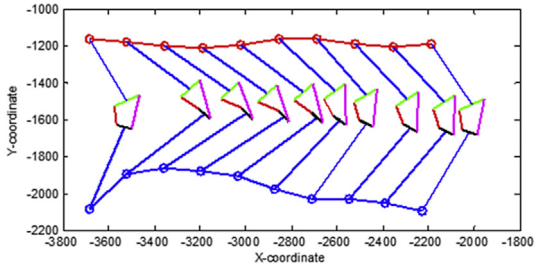

Figure 12 Stick diagram of 4-bar linkage lower limb exoskeleton for one gait cycle.

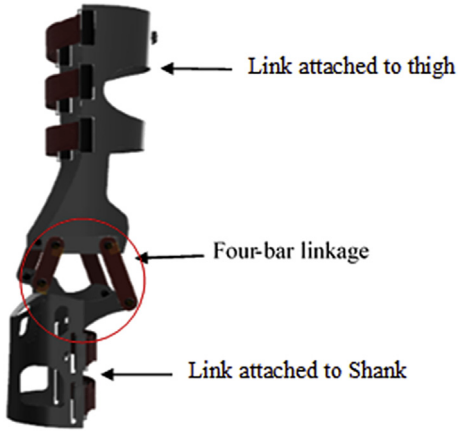

Figure 13 Conceptual design of 4-bar knee exoskeleton.

the orthotic and portable gait rehabilitation devices. The novel gait-based 4-bar linkage synthesis procedure can be used to synthesize any mechanism which involves human walking. The real trajectories are taken with respect to a global reference frame. A total of 10 precision points are selected of 68 points available on the foot and hip trajectories for the synthesis. The ankle trajectory is taken as input, whereas the linkage is designed for tracking the hip trajectory. The synthesis procedure divides the problem into two stages. The first stage is devoted to the linkage design in which five precision points are considered to obtain the linkage parameters. The parameters obtained in the first stage are used as input to the second stage for determining the linkage positions for the remaining five precision points. A two-stage optimization problem is formulated to minimize the tracking error between the generated and desired hip trajectories. To solve this optimization problem, two nature-inspired optimization algorithms, namely, TLBO and PSO are used. It is found that minimum error of 5.2×10^{-2} and 9.92×10^{-8} are obtained during first and second stages, respectively. The designed linkage is simulated in MATLAB for one gait cycle, which is shown in stick diagram.

The proposed gait-based synthesis procedure has been applied on the real trajectories for the first time in this study. This synthesis procedure develops a generalized

walking mechanism for use in the lower limb of exoskeletons, bipeds, prosthesis, rehabilitation devices, etc. The designed mechanism can be integrated with the control technology for its application in gait rehabilitation devices, exoskeleton, bipeds, etc., wherever walking like humans is needed. Besides, this mechanism can also be applied to any body weight support- or portable-rehabilitation devices. The designed linkage can achieve all the orientations required during walking, which is demonstrated through stick diagram.

Figure 13 shows the conceptual design of an exoskeleton device which demonstrates the assembly of the 4-bar linkage. The thigh and shank link lengths in the exoskeleton can be varied to obtain another variant of the exoskeleton; however, these lengths should not exceed the design lengths proposed in this study. This way the proposed mechanism can be embedded in other orthotic/exoskeleton and gait rehabilitation devices. The study can be extended by, considering compliant links in place of rigid links, considering adjustable 4-bar linkage, and use of control technology to embed the designed mechanism in the gait rehabilitation device.

Conflict of interest

The authors declared no potential conflicts of interest with respect to the research, authorship, and/or publication of this article.

Funding

The PhD Scholarship granted by the Ministry of Human Resource Development, Government of India to the first author is highly acknowledged.

Appendix 1

A. Solution of loop closure: The loop closure equation for 4-bar linkage (Figure 4b) can be rewritten in the scalar form as [35]:

$$r_2\cos(\theta_2)+r_3\cos(\theta_3)-r_1\cos(\theta_1)-r_4\cos(\theta_4) \quad (A1)$$

$$r_2\sin(\theta_2)+r_3\sin(\theta_3)-r_1\sin(\theta_1)-r_4\sin(\theta_4) \quad (A2)$$

Squaring and adding Eqs. (A1) and (A2) generate the expression for θ_4. Dividing Eqs. (A2) and (A1) generates the expression for θ_3.

$$\theta_4=2\tan^{-1}\left(\frac{-B_1+\sigma\sqrt{\left(B_1^2-C_1^2+A_1^2\right)}}{C_1-A_1}\right)$$

$\sigma=\mp$, for open and cross assembly mode

$$A_1=2(r_1r_4\cos(\theta_1)-r_2r_4\cos(\theta_2))$$

$$B_1=2(r_1r_4\sin(\theta_1)-r_2r_4\sin(\theta_2))$$

$$C_1=r_1^2+r_2^2+r_4^2-r_3^2-2r_1r_2(\cos(\theta_1)\cos(\theta_2)+\sin(\theta_1)\sin(\theta_2))$$

$$\theta_3=\tan^{-1}\frac{r_1\sin(\theta_1)+r_4\sin(\theta_4)-r_2\sin(\theta_2)}{r_1\cos(\theta_1)+r_4\cos(\theta_4)-r_2\cos(\theta_2)}$$

References

[1] Chen G, Chan CK, Guo Z, Yu H. A review of lower extremity assistive robotic exoskeletons in rehabilitation therapy. Crit Rev Biomed Eng 2013;41(4–5):343–63. https://doi.org/10.1615/CritRevBiomedEng.2014010453.

[2] Ji Z, Manna Y. Synthesis of a pattern generation mechanism for gait rehabilitation. J Med Devices 2008;2. https://doi.org/10.1115/1.2975964. 031004-4-8.

[3] Riener R, Lünenburger L, Jezernik S, Anderschitz M, Colombo G, Dietz V. Patient-cooperative strategies for robot-aided treadmill training: first experimental results. IEEE Trans Neural Syst Rehabil Eng 2005;13(3):380–94. https://doi.org/10.1109/TNSRE.2005.848628.

[4] Chen G, Qi P, Guo Z, Yu H. Mechanical design and evaluation of a compact portable knee-ankle-foot robot for gait rehabilitation. Mech Mach Theory 2016;103:51–64. https://doi.org/10.1016/j.mechmachtheory.2016.04.012.

[5] Pennycott A, Wyss D, Vallery H, Klamroth-Marganska V, Riener R. Towards more effective robotic gait training for stroke rehabilitation: a review. J NeuroEng Rehabil 2012;65(9):1–13. https://doi.org/10.1186/1743-0003-9-65.

[6] Fisher S, Lucas L, Thrasher TA. Robot-assisted gait training for patients with hemiparesis due to stroke. Top Stroke Rehabil 2011;18(3):269–76. https://doi.org/10.1310/tsr1803-269.

[7] Veneman JF, Kruidhof R, Hekman EEG. Design and evaluation of the LOPES exoskeleton robot for interactive gait rehabilitation. IEEE Trans Neural Syst Rehabil Eng 2007;15(3):379–86. https://doi.org/10.1109/TNSRE.2007.903919.

[8] Banala SK, Agrawal SK, Scholz JP. Active leg exoskeleton (alex) for gait rehabilitation of motor-impaired patients. In: Proceedings of the 10th IEEE International conference on rehabilitation robotics, 2007 Jun 12–15. The Netherlands: Noordwijk aan Zee; 2007. p. 401–7.

[9] Tsuge BY, McCarthy JM. An adjustable single degree of freedom system to guide natural walking movement for rehabilitation. J Med Devices 2016;10. https://doi.org/10.1115/1.4033329. 044501-1-6.

[10] Strausser KA, Kazerooni H. The development and testing of a human machine interface for a mobile medical exoskeleton. In: IEEE/RSJ International conference on intelligent robots and systems, 2011 September 25–30; 2011. p. 4911–6. https://doi.org/10.1109/IROS.2011.6095025.

[11] Esquenazi A, Talaty M, Packel A, Saulino M. The ReWalk powered exoskeleton to restore ambulatory function to individuals with thoracic-level motor-complete spinal cord injury. Am J Phys Med Rehabil 2012;91(11):911–21. https://doi.org/10.1097/PHM.0b013e318269d9a3.

[12] Quintero HA, Farris RJ, Goldfarb M. A method for the autonomous control of lower limb exoskeletons for persons with paraplegia. J Med Devices 2012;6(4):0410031–6. https://doi.org/10.1115/1.4007181.

[13] Neuhaus PD, Noorden JH, Craig TJ. Design and evaluation of Mina: a robotic orthosis for paraplegics. In: IEEE International conference on rehabilitation robotics, 2011, June 29–July 1, Zurich, Switzerland; 2011. p. 870–7. https://doi.org/10.1109/ICORR.2011.5975468.

[14] Hirschmann MT, Müller W. Complex function of the knee joint: the current understanding of the knee, knee surgery, sports traumatology. Arthroscopy 2015;23(10):2780–8.

[15] Menschik A. Mechanik des kniegelenkes. Z Orthop 1974 Jun; 112:481–95.

[16] Sim FH. The knee: form, function, and ligament reconstruction. In: Mayo Clinic Proceedings, Vol. 59; 1984 Jan 31. p. 55. No. 1; [Elsevier].
[17] Hamon A, Aoustin Y, Caro S. Two walking gaits for a planar bipedal robot equipped with a four-bar mechanism for the knee joint. Multibody Syst Dyn 2014;31(3):283—307.
[18] Hamon A, Aoustin Y. Cross four-bar linkage for the knees of a planar bipedal robot. In: Humanoid Robots (Humanoids), 2010 10th IEEE-RAS International conference on 2010 Dec 6. IEEE; 2010. p. 379—84.
[19] Aoustin Y, Hamon A. Human like trajectory generation for a biped robot with a four-bar linkage for the knees. Robotics Aut Syst 2013;61(12):1717—25.
[20] Hamon A, Aoustin Y. Study of different structures of the knee joint for a planar bipedal robot. In: Humanoid Robots, 2009. Humanoids 2009. 9th IEEE-RAS International conference on 2009 Dec 7. IEEE; 2009. p. 113—20.
[21] Jin D, Zhang R, Wang R, Zhang J. Kinematic and dynamic performance of prosthetic knee joint using six-bar mechanism. J Rehabil Res Dev 2003;40(1):39—48.
[22] Kora K, Stinear J, McDaid A. Design, analysis, and optimization of an acute stroke gait rehabilitation device. J Med Devices 2017;11(1):014503.
[23] Low KH, Yin Y. Providing assistance to knee in the design of a portable active orthotic device. In: Automation Science and Engineering, 2006. CASE'06. IEEE International conference on 2006 Oct 8. IEEE; 2006. p. 188—93.
[24] Singh R, Chaudhary H, Singh AK. Defect-free optimal synthesis of crank-rocker linkage using nature-inspired optimization algorithms. Mech Mach Theory 2017;116:105—22. https://doi.org/10.1016/j.mechmachtheory.2017.05.018.
[25] Kim H, Lee J, Jang J, Han C, Park S. Mechanical design of an exoskeleton for load carrying augmentation. In: IEEE robotics (ISR) 44th international symposium, 2013 October 24—26; 2013. p. 1—5. https://doi.org/10.1109/ISR.2013.6695682.
[26] Kim H, Park S, Han C. Design of a novel knee joint for an exoskeleton with good energy efficiency for load-carrying augmentation. J Mech Sci Technol 2014;28(11):4361—7. https://doi.org/10.1007/s12206-014-1003-8.
[27] Guo Z, Yu H, Yin YH. Developing a mobile lower limb robotic exoskeleton for gait rehabilitation. J Med Devices 2014;8(4):044503.
[28] Al-Araidah O, Batayneh W, Darabseh T, Banihani SM. Conceptual design of a single DOF human-like eight-bar leg mechanism. Jordan J Mech Ind Eng 2011;5(11):285—9.
[29] Jun S, Zhou X, Ramsey DK, Krovi VN. Kinetostatic design-refinement of articulated knee braces. In: ASME proceedings of International design engineering technical conference and computers and information in engineering conference, 2013, August 4—7; 2013. https://doi.org/10.1115/DETC2013-12716.
[30] Tsuge BY, Plecnik MM, McCarthy JM. Homotopy directed optimization to design a six-bar linkage for a lower limb with a natural ankle trajectory. J Mech Robotics 2016;8(6):061009. https://doi.org/10.1115/1.4034141.
[31] Tsuge BY, McCarthy JM. Synthesis of a 10-bar linkage to guide the gait cycle of the human leg. In: Proceeding of ASME 2015 International design engineering technical conferences and computers and information in engineering conference 2015 Aug 2; 2015. p. 2—5.
[32] Ghosh S, Nina R, McCarthy JM. Geometric design of a passive mechanical knee for lower extremity wearable devices based on anthropomorphic foot task geometry scaling. In: ASME 2015 International design engineering technical conferences and computers and information in engineering conference. American Society of Mechanical Engineers; 2015.
[33] Prakash C, Gupta K, Mittal A, Kumar R, Laxmi V. Passive marker based optical system for gait kinematics for lower extremity. In: International conference on advanced computing technologies and applications, procedia computer science, vol. 45; 2015. p. 176—85. https://doi.org/10.1016/j.procs.2015.03.116.
[34] Norton RL. Kinematics and dynamics of machinery. India: McGraw-Hill; 2010. ISBN: 0-07-0144480-X.
[35] Waldron KJ, Kinzel GL. Kinematics, dynamics, and design of machinery. John Wiley & Sons; 1999.